Environmental Engineering and Management Journal

May 2020, Vol. 19, No. 5, 773-783
http://www.eemj.icpm.tuiasi.ro/; http://www.eemj.eu

"Gheorghe Asachi" Technical University of Iasi, Romania

AN EXPERIMENTAL STUDY ON MECHANICAL AND THERMAL BEHAVIOR OF ACRYLONITRILE BUTADIENE STYRENE ENHANCED WITH FIRE RETARDANTS

Tudor Mihai Simionescu[1], Iuliana Spiridon[2], Cristian Dragoș Varganici[2], Raluca Nicoleta Darie-Nita[2], Alina Adriana Minea[1]*

[1]"Gheorghe Asachi"Technical University of Iasi, Faculty of Materials Science and Engineering, 59 D. Mangeron Blvd., 700050, Iasi, Romania
[2]"Petru Poni" Institute of Macromolecular Chemistry, 41A Gr. Ghica Voda Alley, 700487, Iasi, Romania

Abstract

Nine samples of recycled acrylonitrile butadiene styrene (ABS) with organic montmorillonite and fire retardants adding were combined to prepare ABS copolymer nanocomposites. A very good dispersion of clay and fire retardant was noticed in the recycled ABS (reABS) matrix. The effect of montmorillonite and fire retardants on the mechanical and thermal properties of the reABS nanocomposites was further investigated. Experimental results showed that the addition of organic montmorillonite increased the Young modulus and decreased the tensile strength. As a conclusion of mechanical tests it can affirm that the best overall mechanical results are obtained for reABS 1% OMT 18% FR. The thermal analysis clearly shows that the reABS-OMT-FR nanocomposites have higher thermal stability than the pure reABS. Also, the reABS-OMT-FR char mass and the glass transition temperature are larger than those for pure reABS.

Key words: acrylonitrile butadiene styrene (ABS), DSC, fire retardant, mechanical, montmorillonite, TGA

Received: May, 2019; Revised final: November, 2019; Accepted: December, 2019; Published in final edited form: May, 2020

1. Introduction

Plastics, namely ABS (acrylonitrile butadiene styrene), are used for the manufacture of many components and products, as for example: child safety seats and airbags in the automobiles, parts of roofs, walls and buildings energy efficient insulation (Ford and Fisher, 2019; Masukume et al., 2017). So, all these plastics around us actually are increasing the risks in case of a fire scenario, so any slight improvement may control the damages in a large fire situation. Besides, reusing ABS to create recycled ABS (reABS) is becoming progressively widespread as virgin ABS can demonstrate to be expensive as a raw material (Charles et al., 2019; Tiuc et al., 2016). The entire process can be summarized as: the used ABS is first shredded with the recovered ABS then used with virgin ABS to produce a new product (Singh et al., 2019). Beyond the desirable material properties, ABS manufacturing processes can be summarized as: casting, CNC machining, laser ablation/engraving, injection molding, and 3D printing (Mohammed et al., 2019). In this idea, the recycled acrylonitrile butadiene styrene (reABS) is also suited for 3D printing and is largely used as unique co-polymer or in several combinations due to its intrinsic properties like good mechanical and chemical properties, reduced specific weight and facile processing (Balazs et al., 1998; Balazs et al., 1999; Bardziński, 2014; Fredrickson and Bicerano, 1999; Gilman et al., 2000; Meri et al., 2015; Mohammed et al., 2019; Ray et al., 2002; Vaia et al., 1995; Vaia and Giannelis, 1997a, 1997b). One of its

* Author to whom all correspondence should be addressed: e-mail: aminea@tuiasi.ro

main disadvantages is the high flammability and the toxic smoke as well as its capacity to extent a fire event to its vicinities (Balazs et al., 1998; Ray et al., 2002).

On the other hand, additives are extremely important in determining polymers final properties. Nevertheless, the addition of additives in polymers is severely controlled by regulatory institutions due to global efforts to decrease the use of environmentally unfavorable and health threatening materials (Meri et al., 2015). Therefore, it is of great importance to develop environmentally safe additives for polymers. In this idea, montmorillonite nanoclays offer great benefits mainly because of availability of resources and reasonable price and in connection with the beneficial technological characteristics (nanodimensions, high aspect ratio, and outstanding exploitation properties) (Hense et al., 2015; Meri et al., 2015).

Montmorillonite is one of the best option for filler material in reABS, being a natural mineral that forms alumina silicate layers (Bardziński, 2014; Spranceana et al., 2017). The organic modified montmorillonite (OMT) can be obtained by ion exchange between the montmorillonite and C_{16} in water, method that was detailed by Vaia et al. (1995). Plus, its presence in ABS improves the mechanical properties (Meri et al., 2015; Vaia and Giannelis, 1997b), thermal properties (Balazs et al., 1998; Balazs et al., 1999) and also the fire behavior (Costiuc et al., 2015; Fredrickson and Bicerano, 1999).

Lately, an increased attention was focused on polymers combined with nanocomposites and was demonstrated the adding up to 10% nanoclay in basic polymers can lead to a significant escalation in thermal and mechanical properties of the hybrid material (Fredrickson and Bicerano, 1999; Khobragade et al., 2016; Mahanta et al., 2012; Mao et al., 2016; Paul and Robeson, 2008). More precisely, Mao et al. (2016) manufactured a hybrid material by adding nitrile rubber and montmorillonite Nanofil 15 in reABS and concluded that the new hybrid material has improved thermal properties and good results in mechanical tests.

Zhang et al. (2006) mixed ABS with Triclay III (30 g MMT în 500 ml THF/H20 for three hours to obtain a good dispersion and concluded that the final mechanical properties were affected by the clay percentage. Precisely, the Young modulus increased with the Triclay III percentage while the elongation decreased drastically.

Modesti et al. (2007) studied a nanocomposite based on ABS improved with Bentone 108 and Dellite 43B and found that the elastic modulus is highly influenced by the additive content. Tirantili et al. (2011) studied a nanocomposite ABS -OMT Cloisite 30B and determined that the mechanical stress is not affected by clay percentage while noticed an increase of Young modulus and a substantial decrease (up to 50%) of the elongation with the upsurge of OMT percentage.

Nevertheless, other authors (Cao et al., 2017; Cuppoletti, 2011; Hong et al., 2014, Jian et al., 2014; Liang et al., 2009; Liu, 2014; Malas et al., 2014; Pour et al., 2015; Rahimi et al., 2014; Realinho et al., 2018; Stanciu et al., 2009; Wang et al., 2003; Weng et al., 2016) managed to improve the tensile and the impact strength of ABS by adding clays or nanoparticles. Hong et al. (2014) manufactured ABS + graphene nanosheets + three metal hydroxide nanorods and noticed an improved of tensile strength for the improved ABS at 43.1 MPa for the ABS 1wt% GNS 4%wt. $Co(OH)_2$ and attributed this enhancement to the 3D network acquired from homogenous dispersion of graphene and $Co(OH)_2$.

Liu (2014) analyzed the effect of introducing nanoclay montmorillonite, flame retardant magnesium hydroxide (MH) and compatibilizer LDPE grafted maleic anhydride (LDPE-g-MA) into LDPE and cross-linked polyethylene (XLPE) as the matrix. The conclusion was that the tensile and impact strengths were enhanced by adding LDPE-g-MA and clay (Liu, 2014). Rahimi et al. (2014) studied the recycled ABS properties and found that both the yield stress of tensile tests and Young's modulus are enhanced by 2% in comparison with pure ABS. Cao et al. (2017) performed TG and FTIR analysis that indicated that Hexakis (4-nitrophenoxy) cyclotriphosphazene and ammonium polyphosphate promoted the form of cross-link structure in the ABS, which acted as a barrier near the surface of material.

A way to enhance the mechanical properties of the ABS was studied by Wu and Lang (2016), who introduced ethylene-co-acrylic ester-co-glycidyl methacrylate in poly composite PC/ABS (50/50) with aluminum hypophosphite as fire retardant. The conclusion was that the elongation was increased at 23 % and the impact strength by 2.5 times.

In regard to thermo gravimetrical analysis, Mahanta et al. (2012) compared the ABS and reABS thermal stability and found that $T_{5\%}$ is decreasing from 273 °C (for the ABS) to 201°C for the reABS. However, other authors (Du et al., 2010; Jian et al., 2014; Ma et al., 2008; Realinho et al., 2018; Singh and Ghosh, 2014) found higher temperatures, as for example 377°C (Du et al., 2010) or 378 °C (Jian et al., 2014). Considering the state of the art, this present work investigates mechanical and thermal behavior of recycled ABS by adding different mass fractions of organic montmorillonite nanoparticles and fire retardants.

2. Experimental work

2.1. Materials

The matrix for the experimental study was recycled ABS (reABS) and two types of EXOLIT were selected as fire retardants. Plus, montmorillonite nanoparticles were considered as fillers. reABS was purchased from S.C. Romcarbon S.A. (Buzau, Romania) in granule form with characteristics provided in Table 1.

Table 1. Properties of reABS - Rocadur RABS 52

Melt flow index at 230º C	5 g/10 min
Notched Izod Impact Strength (23°C)	8 kJ/ m^2
Tensile Stress at 23 °C	38 MPa
Tensile strain at 23 °C	2.2 %
Tensile modulus	2363 MPa
Density	1.03 kg/m^3
Heat Deflection Temperature	80°C

The two phosphorus flame retardant additives are: ammonium polyphosphate (APP), Exolit® AP422, and aluminum diethylphosphinate (AlPi), Exolit® OP1230, both supplied, in form of white powder, by Clariant (Germany) with the properties in Table 2, as per given by the manufacturer. The two FR will be used in manufacturing the samples in a 1:1 proportion, as was recommended by the manufacturer. In addition, nanoparticles of organic montmorillonite (OMT) with the commercial name Shelsite 30B Montmorillonite Nanoparticles (Nanoshell) was used as clay for preparing the samples and properties are in Table 3.

Table 2. Properties of FR

	Exolit OP 1230	***Exolit AP 422***
Chemical formula	[(C2H5)2PO2]3 Al	(NH4PO3)n
Phosphor content, %	23.3-24 %	31-32 %
Humidity, %	max. 0.2 %	max. 0.25 %
Density, g/cm^3	1.35	1.9
Decomposing temperature, °C	>300	> 275
Particle dimension	20-40 μm	17 μm

Several formulations were prepared (see Table 4) and all the materials were initially dried at 100°C for 24 hours. Compounding was performed at 205 °C for 10 min, at a rotation speed of 60 rpm, using a fully automated laboratory Brabender station (Brabender, Germany). For mechanical characterization, specimens were prepared by compression molding using a Carver press at 205 °C (with a pre-pressing step of 3 min at 50 atm and a pressing step of 2 min at 150 atm).

The samples structure was selected based on recommendations from the previous published literature, aiming to study the influence of OMT and FR percentages on mechanical and fire properties.

Table 3. Properties of OMT

Formula	MT2OtOH
Particle dimension	< 80 nm
Purity	99 %
SSA (BET)	50-70 m^2/g
Refraction index	1.47
PH	8 - 9
MOHS hardness	5.5
Mass loss after burning	30 %
Humidity	< 2%
Density	2.8 g/cm^3

2.2. Measurements and characterization

The tensile strength of all samples was evaluated by an Instron equipment of 1 KN (Instron Inc., USA) and a speed of 10 mm/min on 55 x 10 x 10 mm samples that were prepared according to the EN ISO 527:2012 standards. The Charpy impact strength of all samples was measured according to EN ISO 179:2001 standard, using a CEAST equipment (Instron Inc., USA) with 50 J energy and an overall accuracy of less than 0.25%, using 83 x 20 x 4 mm probes. At least 3 specimens were verified for each composition (as it is depicted in Table 4) to acquire mean values of mechanical and impact parameters in order to reduce the testing uncertainty.

Differential scanning calorimetric (DSC) measurements were conducted on a NETZSCH DSC 200F3 Maia device (Netzsch, Germany) using a heating rate of 10 °C/min. The equipment has a measurement accuracy of 0.1 K, as declared by the manufacturer. A mass of 10 mg of each sample was heated in pierced and sealed aluminum crucibles in nitrogen atmosphere at a flow rate of 50 mL/min. The temperature against heat flow was recorded.The baseline was obtained by scanning the temperature domain of the experiments with an empty pan. The instrument was calibrated with indium at various heating rates according to standard procedures.

Table 4. Prepared samples

Sample code	***Content (%wt)***			
	reABS	***OMT***	***EXOLIT OP 1230***	***EXOLIT AP 422***
reABS	100.0	-	-	-
reABS 1% OMT	99.0	1.0	-	-
reABS 15% FR	85.0	-	7.5	7.5
reABS 1% OMT 15% FR	84.0	1.0	7.5	7.5
reABS 1% OMT 18% FR	81.0	1.0	9.0	9.0
reABS 1% OMT 20% FR	79.0	1.0	10.0	10.0
reABS 2% OMT	98.0	2.0		
reABS 2% OMT 15% FR	83.0	2.0	7.5	7.5
reABS 2% OMT 18% FR	80.0	2.0	9.0	9.0
reABS 2% OMT 20% FR	78.0	2.0	10.0	10.0

The thermal stability of the samples was performed on a TGA STA 449 F1 Jupiter (Netzsch, Germania), with a TGA resolution of 0.025 µg, as declared by the manufacturer. All samples were heated in alumina crucibles under a 50 ml/min flux of nitrogen atmosphere in the temperature range of 20 - 700 °C at a heating rate of 10 °C/min.

Scanning electron microscopy (SEM) images were acquired using a Hitachi SU 8230 Scanning Electron Microscope (Hitachi, Ltd. Japan) equipped with EDX Oxford detector-analyzer.

3. Results and discussion

3.1. Tensile and impact strength test

All mechanical tests took place at 50% relative humidity (RH) and 23°C. The specimens were conditioned under the same circumstances for 24 h before testing. The results are presented in Table 5 and represent an average for the tested samples and are in line with the open literature (Cao et al., 2017) that acknowledges that the addition of fire retardants to the polymer matrix strongly affects the mechanical properties of the materials.

Results show that adding 15 % fire retardant is decreasing drastically the mechanical properties of the reABS: the elongation is decreasing by three times while tensile strength is decreasing by 25% and Young modulus is increasing from 1888.09 to 2404.56 MPa. If it compares the characteristics of the pure ABS with our reABS it can see that the mechanical performances are decreasing by 10%, fact that is in-line with research performed by Mahanta et al. (2012).

If it further compares our results with those obtained by Tirantilis et al. (2011), one can see that we obtained a decrease in tensile strength of 14 % while other properties are in line with referenced research and an explanation can rely on different base material.

If one considers Table 5, it can be noted a small increase in Young modulus and a decrease in tensile strength when OMT is added to the reABS. This can be due to a good dispersion of OMT nanoparticles in the reABS matrix (Liang et al., 2009; Malas et al., 2014; Pour et al., 2015). Plus, when both OMT and fire retardant are added the Young modulus is increasing, but the tensile strength is decreasing at 21.74 MPa. This can be due to plasticization caused by the mobility restraining of ABS chains when organic montmorillonite nanocomposite is added. Nevertheless, some contradictory information was noticed in the literature (Weng et al., 2016) and can be explained by the differences in OMT structure that can favor a better dispersion of it in the matrix structure. Therefore, the best overall mechanical results were obtained for reABS 1% OMT 18% FR.

As regards the impact strength, a severe decrease with about 60-65 % was noticed when FR and OMT are added into the reABS matrix, but if compares all the data from Table 5, it can say that the reABS 1% OMT 18% FR got a good result at impact in comparison with the other reABS+OMT+FR samples. Similar decrease was noticed also in the literature (Liu, 2014).

If it further discusses the Young modulus, that measures the stiffness of a solid material, in Fig. 1 it can easily notice the influence of both OMT and FR on this mechanical property. From Fig. 1 it can be noted that the Young modulus is increasing with both FR and OMT mass fraction in the reABS matrix. The surface that approximates the experimental points in the 3D plot has an R-squared value of 0.972 and reflects very well the changes in Young modulus when the reABS matrix contains nanocomposites and/or fire retardants. More exactly, the Young modulus is increasing by 27% if 15% fire retardant is added to the reABS matrix and goes to 37% if OMT is also added. On the other hand, the OMT influence is also relevant, going to an upsurge of 11% in Young modulus, but the most relevant effect on stiffness is obtained by combining nanocomposites with fire retardants.

3.2. Thermal analysis

The thermal stability of samples was first investigated by thermogravimetric analysis (TGA) on few samples and the results are shown in Table 6. The reABS samples decomposed in just one stage at maximum 425 °C and a mass loss of 92%, with 5% ($T_{5\%}$) and maximum mass loss rate (T_{peak}) taking place at 355 °C and 472 °C, respectively. Plus, similar findings were noticed also by Realinho et al. (2018).

Table 5. Mechanical properties of composite materials

Sample code	*Young modulus, MPa*	*Tensile strength, MPa*	*Elongation at break, mm*	*Impact strength, KJ/m²*
reABS	1888.09	31.25	2.99	20.28
reABS 15% FR	2404.56	24.26	0.76	7.14
reABS 2% OMT	2102.46	27.26	1.30	8.84
reABS 2% OMT 15% FR	2587.61	21.71	0.47	5.43
reABS 2% OMT 18% FR	2507.32	21.14	0.44	5.39
reABS 2% OMT 20% FR	2570.38	18.50	0.35	5.51
reABS 1% OMT	1926.36	27.06	1.99	7.69
reABS 1% OMT 15% FR	2274.15	21.74	0.76	4.39
reABS 1% OMT 18% FR	2346.42	22.59	0.77	6.75
reABS 1% OMT 20% FR	2465.86	22.16	0.53	6.09

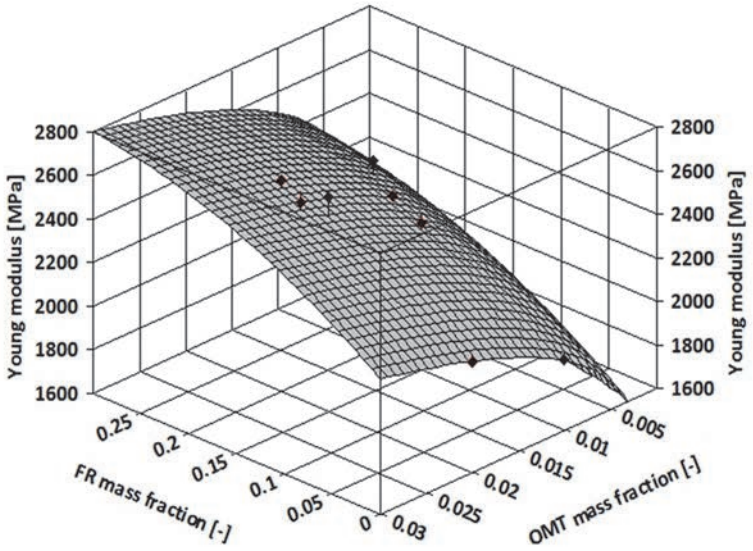

Fig. 1. Variation of Young modulus for reABS matrix samples

Addition of organic nanoparticles and fire retardant (i.e. mixture of APP and AlPi, with mass ratio of 1:1) delays the decomposition and decreased the mass loss, as can be noted from Table 6 and Fig. 2. More precisely, reABS-OMT-FR samples decomposed in two steps (as one can note from Table 6). The first decomposition step occurred around 344-373 °C with a mass loss of about 12-19%, while the second stage occurred at about 470°C with a mass loss of maximum 68%.

Fig. 2 depicts the mass loss over temperature and in Fig. 3 are the DTG results, where the derivative curves will characterize the degradation, represented as peaks. The experimental data investigation clearly shows that the reABS-OMT-FR nanocomposites have higher thermal stability than the pure reABS sample, as will be argued further on. Additionally, the performance of these new nanocomposites will be discussed in comparison with that of reABS and one can observe a noteworthy interaction between reABS and FR. This interaction take place by influencing the decomposition of reABS (see Fig. 2). Comparable conclusions were stated also by Pawlowski and Schartel (2007) in their study about ABS and GNP incorporation in the matrix. As is depicted in Fig. 2 and Fig. 3, all manufactured samples displayed higher thermal stability as compared to reABS, and the incorporation of OMT-FR yield in a significant thermal stability enhancement of the nanocomposites. If it discusses Fig. 2, the mass loss by adding low percentages of OMT (i.e. 1% OMT) is going to maximum 20.33%, while a 2%OMT goes to a mass loss increase at 22.09%, both measured at 694 °C. This clearly indicates that the addition of OMT and FR increases the mass loss heat behavior by 2.67-3.15 times, depending on the concentration of the additives.

A similar phenomenon can be observed also from the DTG results (see Fig. 3), concluding that the addition of OMT and FR slightly changes the major degradation peak temperature (i.e. about 7-10 °C). Also, the degradation for all studied materials take place in just one phase. Concluding, these experimental observations clearly shows that the OMT+FR increases the thermal stability of the reABS.

If it discusses about the char resulted from the process, it can be noted an increase of about 11-15 % (see Table 6) when OMT_FR are added in the reABS matrix. This upsurge can be attributed to increased thermal stability of the reABS-OMT-FR samples and formation of a network of char layers during combustion that retards the out-diffusion of gaseous decomposition products, as was noticed also by Pour et al. (2015). In regard to state of the art, also previous experiments on graphene/Polyvinyl alcohol performed by Liang at al. (2009) showed and enhancement of the nanocomposite's thermal stability due to the formation of char layer that offers polymer thermal lagging.

Furthermore, a DSC study was performed for the reABS-OMT-FR samples and results (see Fig. 4 and Table 7) shows the glass transition temperatures (T_g) of the samples.

The glass transition temperature, usually named T_g, is a very important property of polymers for a certain application. Glass transition temperature is the temperature, below which the physical properties of plastics change to those of a glassy or crystalline state. Over T_g they perform similar to any rubbery materials. Beneath T_g a plastic's molecules have moderately low mobility. Also, polymers properties can be radically dissimilar at temperatures up or below T_g.

In this study, the differential scanning calorimetry (with an accuracy of 0.1 K, as declared by the manufacturer) was considered for this purpose and the results indicated that T_g is increasing by adding both OMT and FR by 3-10%. The maximum increase was noticed for the reABS 2% OMT 20% FR, indicating an increased rigidity of the polymer chain if compared to reABS.

Table 6. Data extracted from TGA analysis

Sample	*Stage*	$T_{5\%}$ (°C)	T_{onset} (°C)	T_{max} (°C)	T_{endset} (°C)	W_m (%)	W_{rez} (%)
reABS	I	355	–	425	472	92	6.59
reABS 1% OMT 15% FR	I	323	–	344	392	12.12	18.33
	II	–	392	429	463	67.48	
reABS 1% OMT 20% FR	I	325	–	367	397	16.64	20.09
	II	–	397	429	468	61.34	
reABS 2% OMT 15% FR	I	305	–	370	399	12.46	21.41
	II	–	399	432	471	63.64	
reABS 2% OMT 20% FR	I	336	–	373	403	19.24	21.96
	II	–	403	434	472	57.94	

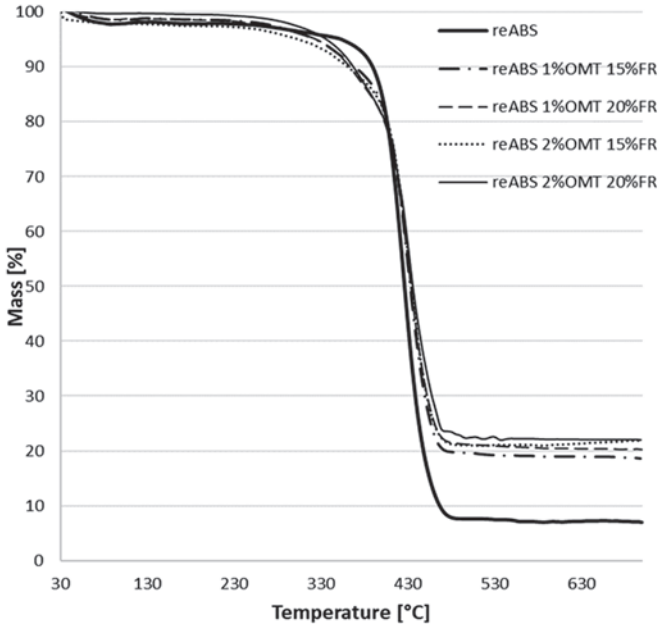

Fig. 2. Mass loss curves of reABS and reABS/OMT/FR nanocomposites

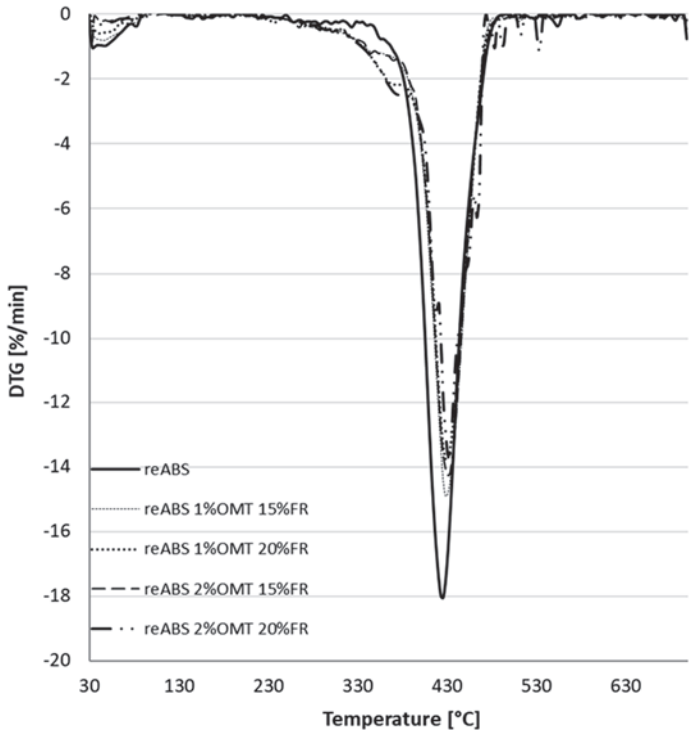

Fig. 3. DTG curves of reABS and reABS/OMT/FR nanocomposites

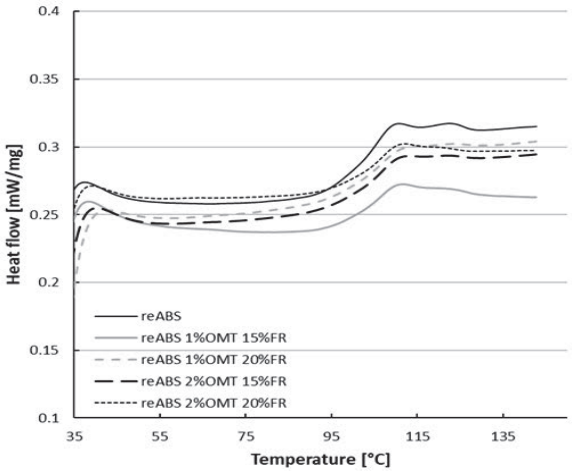

Fig. 4. DSC results of studied samples

Table 7. Glass transition temperatures of manufactured samples

Sample	*Glass transition temperature T_g [°C]*
reABS	100
reABS 1% OMT 15% FR	103
reABS 1% OMT 20% FR	105
reABS 2% OMT 15% FR	108
reABS 2% OMT 20% FR	110

The phase separation of the polymer-nanocomposite-fire retardant system was characterized by the change of the glass transition of reABS. In the case of the reABS-OMT-FR samples, an increase of T_g was detected due to the very good compatibility between the nanocomposite and the reABS matrix. An explanation of the change in T_g values of reABS in the nanocomposites, two contradictory effects of nanofillers were acknowledged in the open literature (Mao et al., 2016): (I) decrease of the molecule mobility owed by the obstructing influence and (II) upsurge of the free volume due to the existence of nanofillers and the untied molecular packing of the chains. On the other hand, our results for the reABS are mostly in line with similar work from other researchers (Mao et al., 2016; Tarantili, 2011). Nevertheless, adding OMT and FR increases the glass transition temperature from 100 to 110°C due to the restrained mobility of the reABS chains because of the fire-retardant action, as was also found by Hong et al. (2007).

3.3. SEM analysis

In order to investigate the detailed dispersion status fillers and clay into the polymer matrix, SEM analysis was performed (Figs. 5-10).

In Figs. 5 - 10 are inserted two SEM images for each sample (the first is obtained using the LA-BSE signal and the second one for HA-BSE). BSE (Backscattering Electron) has high energy comparable to the incident electron; includes compositional surface information, as the BSE yield is proportional to the mean atomic number of the specimen; ~50eV average energy.

The LA-BSE image - LA-BSE(U) gives compositional and topographic information while is less sensitive to specimen charging - up. On the other hand, the HA-BSE image - HA(T) gives rich compositional information and less topographic information. The addition of the fire retardants into the reABS+OMT matrix produced a relevant effect on the phase morphology of the samples. The fire retardants particle size is lower than 20 μm while the montmorillonite nanoparticle is of 80 nm, thus resulting in a good dispersion of particles in the matrix, as can be clearly seen from Fig. 5 -10 for every investigated sample.

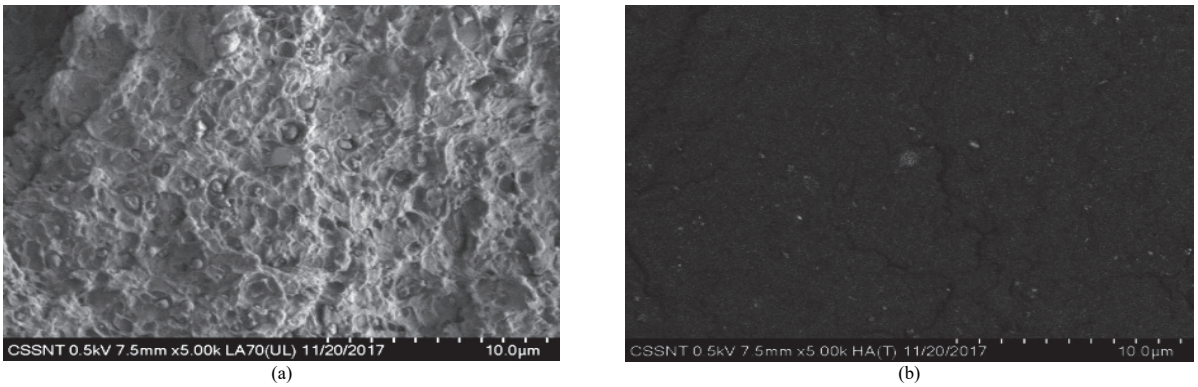

(a) (b)

Fig. 5. SEM images of the reABS samples
(a) image obtained using the LA-BSE signal; (b) image obtained using HA-BSE

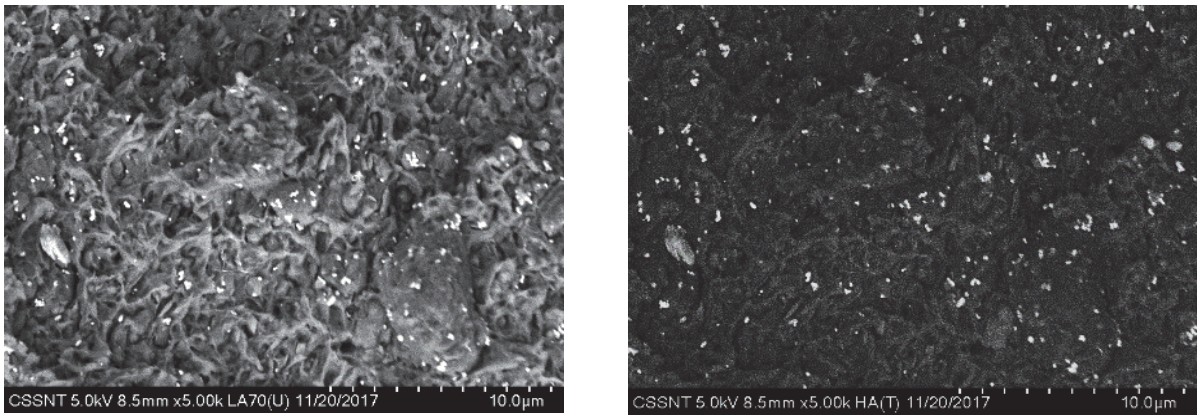

(a) (b)

Fig. 6. SEM images of the reABS1%OMT samples
(a) image obtained using the LA-BSE signal; (b) image obtained using HA-BSE

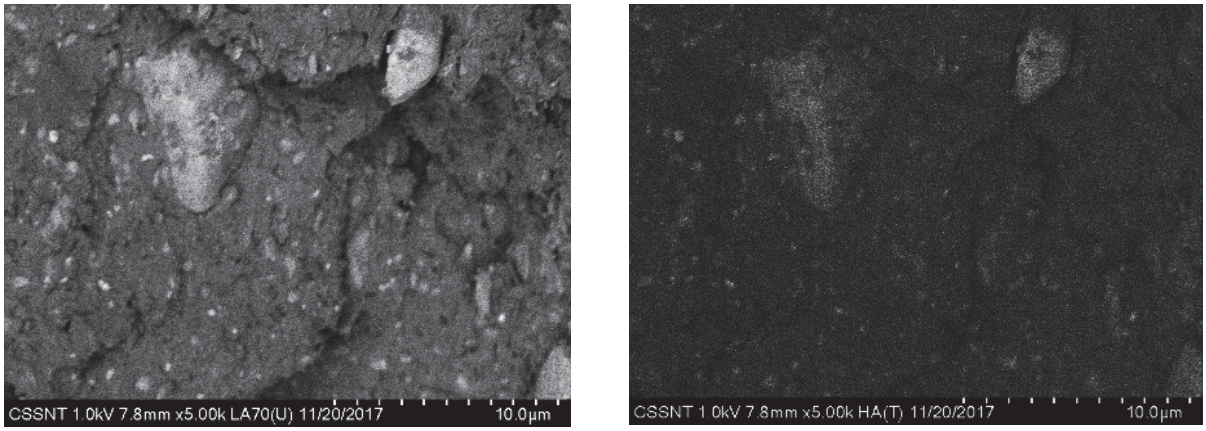

(a) (b)

Fig. 7. SEM images of the reABS1%OMT15%FR samples
(a) image obtained using the LA-BSE signal; (b) image obtained using HA-BSE

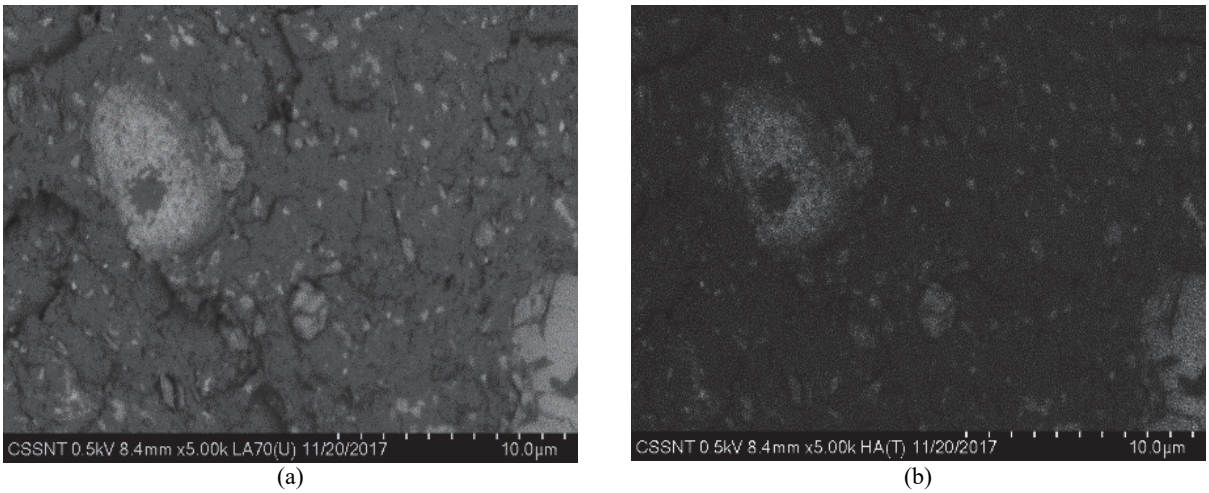

(a) (b)

Fig. 8. SEM images of the reABS1%OMT18%FR samples
(a) image obtained using the LA-BSE signal; (b) image obtained using HA-BSE

If it compares also with open literature results, as Du at al. (2010) noticed, the organic montmorillonite manages to contribute to a better dispersion in comparison with the non-organic one due to its micro spherical structure. Additionally, an upsurge of the surface roughness is noticed due to the dispersion homogeneity of the FR particles into the sample matrix. Similar morphological characteristics was noticed also in some recently reported research performed by Mao at al. (2016) and Kim at al. (2005).

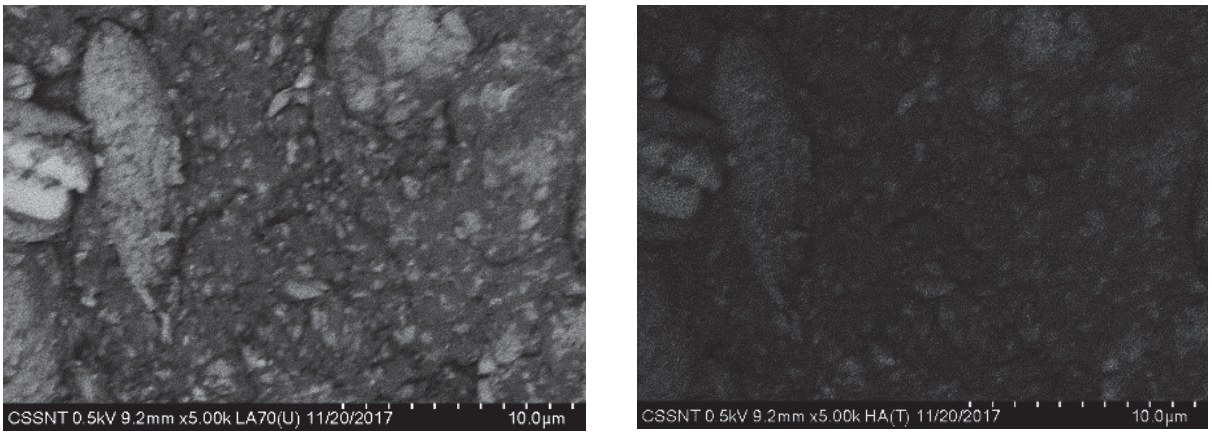

(a) (b)

Fig. 9. SEM images of the reABS2%OMT15%FR samples
(a) image obtained using the LA-BSE signal; (b) image obtained using HA-BSE

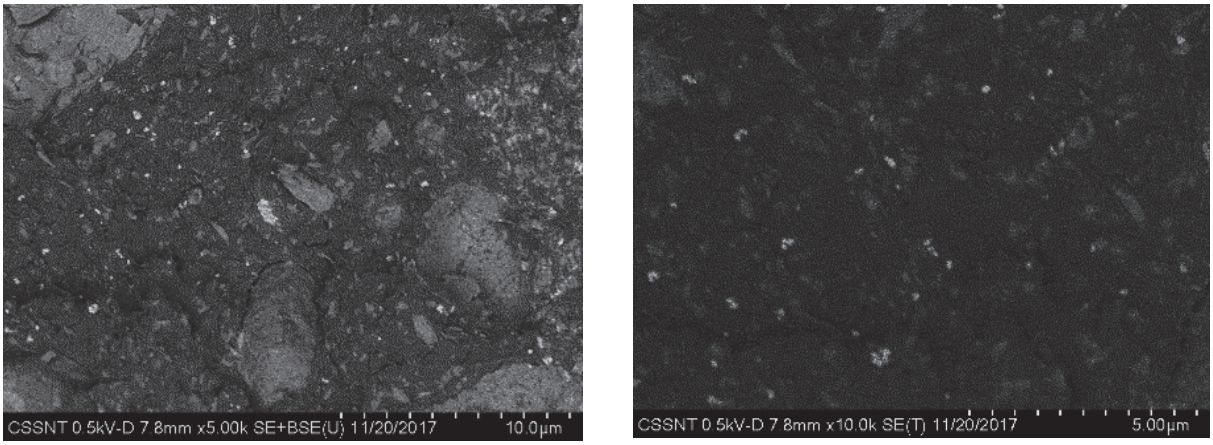

(a) (b)

Fig. 10. SEM images of the reABS2%OMT20%FR samples
(a) image obtained using the LA-BSE signal; (b) image obtained using HA-BSE

4. Conclusions

In this paper the effect of introducing organic montmorillonite and EXOLIT fire retardant into recycled ABS was experimentally studied revealing both mechanical and thermal properties. Consequently, nine samples of copolymer nanocomposites were manufactured and an excellent dispersion of clay and fire retardant in the recycled ABS matrix was noticed.

The conclusions of this experimental study can be summarized as:

- Experimental results of the mechanical tests revealed that the addition of organic montmorillonite increased the Young modulus, while the tensile strength is decreasing. As a conclusion of mechanical tests it can affirm that the best overall mechanical results were obtained for reABS 1% OMT 18% FR.
- Thermal analysis was performed in terms of TGA and DSC and clearly shows that the reABS-OMT-FR nanocomposites have higher thermal stability than the pure reABS. More precisely, the TGA analysis indicated that the char mass is increasing by 11-15% when OMT+FR are added, while DTG curves demonstrated that the reABS-OMT-FR nanocomposites have higher thermal stability than the pure reABS samples.
- DSC analysis confirmed that the glass transition temperature is increasing for the reABS-OMT-FR samples in comparison with pure reABS, making them a better candidate for fire specific applications.

As a main conclusion, reusing ABS and incorporating OMT and fire retardants can create new products that are safer in a fire scenario. Plus, the materials based on reABS are well suited for 3D printing, as was outlined in the state of the art. Nevertheless, more research oriented to a real fire scenario is needed, as well as a cost-benefit analysis that might indicate if the benefits are overcoming the costs.

Nomenclature

$T_{5\%}$ temperature corresponding to 5% mass loss;
T_{onset} onset thermal degradation temperature;
T_{max} temperature that corresponds to the maximum rate of decomposition for each stage;
T_{endset} endset thermal degradation temperature;
W_m mass loss at T_{max};

W_{rez} percentage of residue remained at the end of the thermal degradation process (700°C);

Abbreviations

ABS	acrylonitrile butadiene styrene
AlPi	aluminum diethylphosphinate
APP	ammonium polyphosphate
DSC	differential scanning calorimetry
DTG	derivative thermogravimetry
FR	fire retardant
OMT	organic montmorillonite clay
reABS	recycled acrylonitrile butadiene styrene
RH	relative humidity
SEM	Scanning electron microscopy
TGA	thermogravimetric analysis

References

Balazs A.C., Singh C., Zhulina E., (1998), Modeling the interactions between the polymers and clay surfaces through self-consistent field theory, *Macromolecules*, **31**, 8370-8381.

Balazs A.C., Singh C., Zhulina E., Lyatskaya Y., (1999), Modeling the phase behavior of polymer-clay composites, *Accounts of Chemical Research*, **32**, 651-657.

Bardziński P.J., (2014), On the impact of intermolecular interactions between the quaternary ammonium ions on interlayer spacing of quat-intercalated montmorillonite: A molecular mechanics and ab-initio study, *Applied Clay Science*, **95**, 323-339.

Berthier L., Charbonneau P., Ninarello A., Ozawa M, Yaida S., (2019), Zero-temperature glass transition in two dimensions, *Nature Communications*, **10**, 1-7.

Cao X., Yang Y., Luo H., Cai X., (2017), High efficiency intumescent flame retardancy between Hexakis (4-nitrophenoxy) cyclotriphosphazene and ammonium polyphosphate on ABS, *Polymer Degradation and Stability*, **143**, 259-265.

Charles A., Bassan P.M., Mueller T., Elkaseer A., Scholz S.G., (2019), *On the Assessment of Thermo-Mechanical Degradability of Multi-Recycled Abs Polymer for 3d Printing Aplications*, In: *Sustainable Design and Manufacturing 2019*, Ball P., Huaccho Huatuco L., Howlett R., Setchi R. (Eds.), vol. 155, Springer, Singapore.

Costiuc L., Tierean M., Baltes L., Patachia S., (2015), Experimental Investigation on the heat of combustion for solid plastic waste mixtures, *Environmental Engineering and Management Journal*, **14**, 1295-1302.

Cuppoletti J., (2011), *Nanocomposites and Polymers with Analytical Methods*, Intech Open, Croatia.

Du X., Yu H., Wang Z., Tang T., (2010), Effect of anionic organoclay with special aggregate structure on the flame retardancy of acrylonitrile - butadiene-styrene/clay composites, *Polymer Degradation and Stability*, **95**, 587-592.

Ebnesajjad S., (2016), *Introduction to Plastics*, In: *Plastics Design Library*, *Chemical Resistance of Commodity Thermoplastics*, Baur E., Ruhrberg K., Woishnis W. (Eds.), William Andrew Publishing, 13-25.

Ebnesajjad S., Morgan R., (2019), *Fluoropolymer Additives*, 2nd Edition, William Andrew Publishing, 1-295.

Ford P., Fisher J., (2019), Designing consumer electronic products for the circular economy using recycled Acrylonitrile Butadiene Styrene (ABS): A case study, *Journal of Cleaner Production*, **236**, 117490.

Fredrickson G.H., Bicerano J., (1999), Barrier properties of oriented disk composites, *Journal of Chemical Physics*, **110**, 2181-2188.

Gilman J.W., Jackson C.L., Morgan A.B., Harris Jr.R., Manias E., Giannelis E.P., Wuthenow M., Hilton D., (2000), Flammability properties of polymer-layered silicate nanocomposites. Propylene and polystyrene nanocomposites, *Chemical Materials*, **12**, 1866-73.

Hense P., Reh K., Franke M., Aigner J., Hornung A., Contin A., (2015), Pyrolysis of waste electrical and electronic equipment (WEEE) for recovering metals and energy: Previous achievements and current approaches, *Environmental Engineering and Management Journal*, **14**, 1637-1647.

Hong J.H., Sung Y.T., Song K.H., Kim W.N., Kang B.I., Kim S.L., Lee C.H., (2007), Morphology and dynamic mechanical properties of poly (acrylonitrile-butadiene-styrene)/polycarbonate/clay nanocomposites prepared by melt mixing, *Composite Interfaces*, **14**, 519-532.

Hong N., Zhan J., Wanga X., Stec A.A., Hull T.R., Ge H., Xing W., Song L., Hua Y., (2014), Enhanced mechanical, thermal and flame retardant properties by combining graphene nanosheets and metal hydroxide nanorods for Acrylonitrile-Butadiene-Styrene copolymer composite, *Composites Part A: Applied Science and Manufacturing*, **64**, 203-210.

Jian R.K., Chen L., Chen S.Y., Long J.W., Wang Y.Z., (2014), A novel flame-retardant acrylonitrile-butadiene-styrene system based on aluminum isobutylphosphinate and red phosphorus: Flame retardance, thermal degradation and pyrolysis behavior, *Polymer Degradation and Stability*, **109**, 184-193.

Khobragade P.S., Hansora D.P., Naik J.B., Chatterjee A., (2016), Flame retarding performance of elastomeric nanocomposites: A review, *Polymer Degradation and Stability*, **130**, 194-24.

Kim H.B., Choi J.S., Lee C.H., Lim S.T., Jhon M.S., Choi H.J., (2005), Polymer blend/organoclay nanocomposite with poly (ethylene oxide) and poly (methyl methacrylate), *European Polymers Journal*, **41**, 679-85.

Li T., Wang H., Mays J., Hong K., (2019*), Polymer Structures and Their Glass Transition Temperatures: An Intriguing Relationship*, Conf. APS March Meeting, vol. 64, Boston, Massachusetts.

Liang J., Huang Y., Zhang L., Wang Y., Ma Y., Guo T., (2009), Molecular-Level Dispersion of Graphene into Poly (vinyl alcohol) and Effective Reinforcement of their Nanocomposites, *Advanced Functional Materials*, **19**, 2297-2302.

Liu S.P., (2014), Flame retardant and mechanical properties of polyethylene/ magnesium hydroxide/montmorillonite nanocomposites, *Journal of Industrial and Engineering Chemistry*, **20**, 2401-2408.

Ma H., Tong L., Xu Z., Fang Z., (2008), Intumescent flame retardant-montmorillonite synergism in ABS nanocomposites, *Applied Clay Science*, **42**, 238-245.

Mahanta D., Dayanidhi S.A., Mohanty S., Nayak S.K., (2012), Mechanical, thermal, and morphological properties of recycled polycarbonate/recycled poly (acrylonitrile- butadiene-styrene) blend nanocomposites, *Polymer Composites*, **33**, 2114-2124.

Malas A., Pal P., Das C.K., (2014), Effect of expanded graphite and modified graphite flakes on the physical and thermo-mechanical properties of styrene butadiene rubber/polybutadiene rubber (SBR/BR) blends, *Materials Design*, **55**, 664-673.

Mao N.D., Thanh T.D., Thuong N.T., Grillet A.C., Kim N.H., Lee J.H., (2016), Enhanced mechanical and

thermal properties of recycled ABS/nitrile rubber/nanofil N15 nanocomposites, *Composites Part B:Engineering*, **93**, 280-288.

Masukume M., Onyango M.S., Maree J.P., (2017), Performance characteristics of synthetic zeolite f9 in treating high iron and manganese acid mine drainage, *Environmental Engineering and Management Journal*, **16**, 2255-2265.

Meri R.M., Zicans J., Ivanova T., Berzina R., Saldabola R., Maksimovs R., (2015), The effect of introduction of montmorillonite clay (MMT) on the elastic properties of polycarbonate (PC) composition with acrylonitrile-butadiene styrene (ABS), *Composite Structures*, **134**, 950-956.

Modesti M., Besco S., Lorenzetti A., Causin V., Marega C., Gilman J.W., Fox D.M., Trulove P.C., De Long H.C., Zammarano M., (2007), ABS/clay nanocomposites obtained by a solution technique: Influence of clay organic modifiers, *Polymer Degradation and Stability*, **92**, 2206-2213.

Mohammed M.I., Wilson D., Gomez-Kervin E., Tang B., Wang J., (2019), Investigation of Closed-Loop Manufacturing with Acrylonitrile Butadiene Styrene over Multiple Generations Using Additive Manufacturing, *ACS Sustainable Chemistry & Engineering*, **7**, 13955-13969.

Paul D.R., Robeson L.M., (2008), Polymer nanotechnology: nanocomposites, *Polymer*, **49**, 3187-3204.

Pawlowski K.H., Schartel B., (2007), Flame retardancy mechanisms of triphenyl phosphate, resorcinol bis (diphenyl phosphate) and bisphenol A bis (diphenyl phosphate) in polycarbonate/acrylonitrile-butadiene-styrene blends, *Polymers International*, **56**, 1404-1414.

Pour R.H., Soheilmoghaddam M., Hassan A., Bourbigot S., (2015), Flammability and thermal properties of polycarbonate /acrylonitrilebutadiene- styrene nanocomposites reinforced with multilayer grapheme, *Polymer Degradation and Stability*, **120**, 88-97.

Rahimi M., Esfahanian M., Moradi M., (2014), Effect of reprocessing on shrinkage and mechanical properties of ABS and investigating the proper blend of virgin and recycled ABS in injection molding, *Journal of Materials Processing Technology*, **214**, 2359-2365.

Ray S.S., Yamada K., Okamoto M., Ueda K., (2002), New polylactide/layered silicate nanocomposite: a novel biodegradable material, *Nano Letters*, **2**, 1093-1096.

Realinho V., Haurie L., Formosa J., Velasco J.I., (2018), Flame retardancy effect of combined ammonium polyphosphate and aluminium diethyl phosphinate in crylonitrile-butadiene-styrene, *Polymer Degradation and Stability*, **155**, 208-219.

Singh P., Ghosh A.K., (2014), Torsional, tensile and structural properties of acrylonitrile-butadiene-styrene clay nanocomposites, *Materials and Design*, **55**, 137-145.

Singh R., Singh I., Kumar R., (2019), Mechanical and morphological investigations of 3D printed recycled ABS reinforced with bakelite-SiC-Al2O3, *Proceedings of the Institution of Mechanical Engineers*, *Part C: Journal of Mechanical Engineering Science*, **233**, 5933-5944.

Spranceana A.C., Darie M., Ciausu S., Tudorachi N., Lisa G., (2017), Comparative analysis of thermal stability of building insulation materials, *Environmental Engineering and Management Journal*, **16**, 2831-2842.

Stanciu S., Bujoreanu L.G., Ioniţă I., Sandu A.V., Enache A., (2009), A structural-morphological study of a Cu63Al26Mn11 shape memory alloy, *Advanced Topics of Optoelectronics*, *Microelectronics*, *and Nanotechnologies IV*, **7297**, 1-4.

Tarantili P.A., (2011), *Composites of Engineering Plastics with Layered Silicate Nanofillers: Preparation and Study of Microstructure and Thermomechanical Properties*, In: *Nanocomposites and Polymers with Analytical Methods*, Cuppoletti J. (Ed.), IntechOpen, Rijeka, Croatia.

Tiuc A.E., Dan V., Vermeşan H., Gabor T., Proorocu M., (2016), Recovery of sawdust and recycled rubber granules as sound absorbing materials, *Environmental Engineering and Management Journal*, **15**, 1093-1101.

Vaia R.A., Giannelis E.P., (1997a), Lattice of polymer melt intercalation in organically-modified layered silicates, *Macromolecules*, **30**, 7990-7999.

Vaia R.A., Giannelis E.P., (1997b), Polymer melts intercalation in organically-modified layered silicates: model predictions and experiment, *Macromolecules*, **30**, 8000-8009.

Vaia R.A., Jandt K.D., Kramer E.J., Giannelis E.P., (1995), Kinetics of polymer melts intercalation, *Macromolecules*, **28**, 8080-8085.

Wang S., Hu Y., Lin Z., Gui Z., Wang Z., Chen Z., Fan W., (2003), Flammability and thermal stability studies of ABS/Montmorillonite nanocomposite, *Polymers International*, **52**, 1045-1049.

Weng Z., Wang J., Senthil T., Wu L., (2016), Mechanical and thermal properties of ABS/montmorillonite nanocomposites for fused deposition modeling 3D printing, *Materials and Design*, **102**, 276-283.

Wu N., Lang S., (2016), Flame retardancy and toughness modification of flame retardant polycarbonate/acrylonitrile-butadiene-styrene/AHP composites, *Polymer Degradation and Stability*, **123**, 26-35.

Zhang J., Jiang D.D., Wang D., Wilkie C.A., (2006), Styrenic polymer nanocomposites based on an oligomerically-modified clay with high inorganic content, *Polymer Degradation and Stability*, **91**, 2665-2674.